Contributon Theory for Shielding Analysis

Marat Seydaliev and D.L. Henderson

July 2008

UWFDM-1338

FUSION TECHNOLOGY INSTITUTE

UNIVERSITY OF WISCONSIN

MADISON WISCONSIN

Contributon Theory for Shielding Analysis

Marat Seydaliev and D.L. Henderson

Fusion Technology Institute
University of Wisconsin
1500 Engineering Drive
Madison, WI 53706

http://fti.neep.wisc.edu

July 2008

UWFDM-1338

I. Introduction

Contributon theory, initially introduced by M.L. Williams and colleagues at ORNL [1,2], is a powerful tool for shield design optimization and analysis in nuclear engineering applications. This theory focuses on the so-called "contributon" flux and current of particles, which contribute directly to the detector reading or response of interest. The presence of both the source and the detector establishes a response continuum. Contributon theory treats response flow like fluid flow in a fluid medium and response is carried by special particles called contributons.

II. Theory

The linear Boltzmann transport equation is an integro-differential equation, which describes the neutral particle balance over a spatial domain with the use of appropriate boundary conditions. The solution of this equation is unique; that is, the solution consists of the distribution of particles throughout space, energy and direction. The steady-state Boltzmann equation describing neutral particle transport in a nonmultiplying medium is given by [3]

$$\hat{\Omega}\cdot\vec{\nabla}\psi\left(r,E,\hat{\Omega}\right)+\Sigma_t\left(r,E\right)\ \psi=\int_{E'}\int_{\Omega'}\Sigma\left(r,E'\to E,\hat{\Omega}\to\cdot\hat{\Omega}\right)\ \psi\left(r,E',\hat{\Omega}'\right)\ d\hat{\Omega}'\,dE'+Q\left(r,E,\hat{\Omega}\right) \tag{1}$$

where r = location of the particles,

E = energy of the particles,

$\hat{\Omega}$ = direction of propagation,

$\psi\left(r,E,\hat{\Omega}\right)$ = angular flux at location r, energy R, and direction Ω,

$\Sigma_t\left(r,E\right)$ = total macroscopic cross section,

$\Sigma\left(r,E\to E,\hat{\Omega}\to\hat{\Omega}\right)$ = macroscopic double-differential scatter cross section, and

$Q\left(r,E,\hat{\Omega}\right)$ = a known external source term.

It is convenient to write the transport equation in operator notation as

$$\hat{\Omega}\cdot\vec{\nabla}\psi+B\psi=Q \tag{2}$$

where $B\psi$ is given by

$$B\psi\left(r,E,\hat{\Omega}\right)=\Sigma_t\left(r,E\right)\ \psi\left(r,E,\hat{\Omega}\right)-\int_{E'}\int_{\Omega'}\Sigma\left(r,E'\to E,\hat{\Omega}'\to\hat{\Omega}\right)\ \psi\left(r,E',\hat{\Omega}'\right)\ d\hat{\Omega}'\,dE'\ . \tag{3}$$

Assume that the response observed per unit time is a linear functional of the angular flux

$$R=\left\langle Q^*\left(r,E,\hat{\Omega}\right)\psi\left(r,E,\hat{\Omega}\right)\right\rangle \tag{4}$$

where $Q^*\left(r, E, \hat{\Omega}\right)$ is a known response function indicating how the detector responds to particles at $\left(r, E, \hat{\Omega}\right)$. For example Q^* could be the absorption cross-section. The angle brackets indicate the integration over the space, energy, and direction variables. The streaming term $\hat{\Omega} \cdot \vec{\nabla} \psi$ in Cartesian coordinates can be written as

$$\hat{\Omega} \cdot \vec{\nabla} \psi = \mu \frac{\partial \psi}{\partial x} + \eta \frac{\partial \psi}{\partial y} + \xi \frac{\partial \psi}{\partial z} \tag{5}$$

where $\mu = \cos\theta$.

$\eta = \left(1 - \mu^2\right)^{1/2} \cos\omega$, and

$\xi = \left(1 - \mu^2\right)^{1/2} \sin\omega$.

The angles θ and ω are shown in Fig. 1.

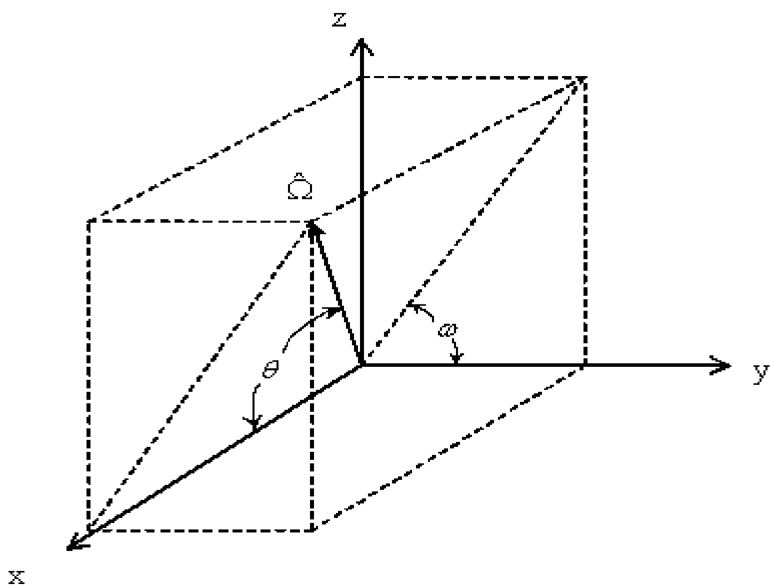

Figure 1. Angular coordinate system.

For two-dimensional Cartesian geometry, there is no z-dependence of the particle flux and the streaming term becomes

$$\hat{\Omega} \cdot \vec{\nabla} \psi = \mu \frac{\partial \psi}{\partial x} + \eta \frac{\partial \psi}{\partial y}. \tag{6}$$

The "importance" of particles throughout the system in contributing to the response corresponds to the adjoint function for this detector, and is given by the adjoint transport equation:

$$-\hat{\Omega}\cdot\vec{\nabla}\psi^*(r,E,\hat{\Omega})+\Sigma_t(r,E)\,\psi^* = \int_{E'}\int_{\Omega'}\Sigma(r,E\to E',\hat{\Omega}\to\hat{\Omega}')\,\psi^*(r,E',\hat{\Omega}')\,d\hat{\Omega}'\,dE'+Q^*(r,E,\hat{\Omega}) \quad (7)$$

or in operator notation:

$$-\hat{\Omega}\cdot\vec{\nabla}\psi^* + B^*\psi^* = Q^* \quad (8)$$

where $B^*\psi^*$ is given by

$$B^*\psi^*(r,E,\hat{\Omega}) = \Sigma_t(r,E)\,\psi^* - \int_{E'}\int_{\Omega'}\Sigma(r,E\to E',\hat{\Omega}\to\hat{\Omega}')\,\psi^*(r,E',\hat{\Omega}')\,d\hat{\Omega}'\,dE'. \quad (9)$$

The adjoint flux can be thought of as the "importance" of a particle at space point r to the detector response. For the forward transport the particles scatter from higher energy groups to lower energy groups, whereas scattering in the adjoint case is from the lower energy groups to the higher energy groups. Therefore the adjoint equation is solved in reverse order with respect to energy. It is also solved in the reverse direction as a function of $-\hat{\Omega}$ rather than $\hat{\Omega}$. In the forward case the particles scatter from $\hat{\Omega}'$ to $\hat{\Omega}$, in the adjoint case the scattering is from $\hat{\Omega}$ to $\hat{\Omega}'$ in the reverse direction. In two-dimensional coordinates the forward direction is defined by η and μ and the adjoint data calculated for that direction will be that appropriate to a particle moving in the direction $(-\mu,-\eta)$.

The importance function $\psi^*(r,E,\hat{\Omega})$, the angular flux $\psi(r,E,\hat{\Omega})$, the source Q, and the detector response function Q^* are interconnected by the relation

$$R = \langle Q^*\psi\rangle = \langle Q\psi^*\rangle. \quad (10)$$

Now by multiplying Eq. (1) by ψ and Eq. (7) by ψ^* and subtracting one can obtain

$$\begin{aligned}&\hat{\Omega}\cdot\vec{\nabla}C(r,E,\hat{\Omega}) + \theta_s(r,E,\hat{\Omega})\,C(r,E,\hat{\Omega}) = \\ &\int_{E'}\int_{\Omega'}\theta(r,E'\to E,\hat{\Omega}'\to\hat{\Omega})\,C(r,E,\hat{\Omega})\,d\hat{\Omega}'\,dE'+S_f(r,E,\hat{\Omega})-S_d(r,E,\hat{\Omega})\end{aligned} \quad (11)$$

where $C(r,E,\hat{\Omega}) = \psi(r,E,\hat{\Omega})\,\psi^*(r,E,\hat{\Omega})$ a new variable – is the angular response flux. This quantity has units of (response/cm^2•eV•sr•s);

$S_f(r,E,\hat{\Omega}) = \psi^*(r,E,\hat{\Omega})Q(r,E,\hat{\Omega})$ = contributon angular response source;

$S_d(r,E,\hat{\Omega}) = \psi(r,E,\hat{\Omega})Q^*(r,E,\hat{\Omega})$ = contributon angular response sink;

$\theta\left(r, E \rightarrow E', \hat{\Omega} \rightarrow \hat{\Omega}'\right) = \Sigma\left(r, E \rightarrow E', \hat{\Omega} \rightarrow \hat{\Omega}'\right) \dfrac{\psi^*\left(r, E', \hat{\Omega}'\right)}{\psi^*\left(r, E, \hat{\Omega}\right)}$ = the double-differential scatter cross section for contributons; and

$\theta_S\left(r, E, \hat{\Omega}\right) = \int\limits_{E'}\int\limits_{\Omega'} \theta\left(r, E \rightarrow E', \hat{\Omega} \rightarrow \hat{\Omega}'\right) d\hat{\Omega}' dE'$ = the total scatter cross section for contributons.

The contributon flux represents the average number of particles at a location *r* moving in the direction $\hat{\Omega}$, which will eventually contribute to the response. Therefore the contributon flux gives the flow rate information for any type of response. Equation (11) appears to be similar to a particle transport equation but with some important distinguishing features. First, there are only scattering reactions in the equation. That means contributons cannot be absorbed. Second, along the vacuum boundaries the angular flux ψ is zero for incoming directions and the adjoint flux ψ^* is zero for outgoing directions. Therefore, the contributon flux must vanish at the vacuum boundaries except for the directions along the boundary. Third, at reflecting boundaries the normal derivatives of ψ and ψ^* vanish; this means that the normal derivative for the contributon flux also vanishes. In other words contributons are reflected back into the system. Therefore contributons can never escape from the system; they originate at the response source S_f and they flow out at the response sink S_d.

Another quantity similar to one in particle transport can be introduced, the angular response current or contributon current. It is defined as follows:

$$\vec{D}\left(r, E, \hat{\Omega}\right) = \hat{\Omega} C\left(r, E, \hat{\Omega}\right) \tag{12}$$

This quantity represents the average flow of contributons moving along the direction of the unit vector $\hat{\Omega}$.

III. Computational Methods

The two-dimensional DANTSYS code system [4] has been used in this work for the calculation of the forward and adjoint directional fluxes. DANTSYS uses the discrete ordinates S_n approximation for the direction variable and a P_l Legendre expansion for the cross sections and angular fluxes. This code solves the neutron and photon transport equation in *(x,y), (r,z)* and (r, θ) geometry with inhomogeneous and fission source options and has several boundary condition options. The code will be used for photon transport. The group structure of photon energies is presented in Table 1. The cross-section data used for the calculations for these energy groups is based on the ENDF/B-VI basic data files. In this case S_{16} approximation and P_5 Legendre expansion were used.

Several auxiliary post-processing codes have been written in FORTRAN that reconstruct the forward angular flux and adjoint angular flux of photons from the DANTSYS output files. These files are RAFLXM, AAFLXM and SNCONS. RAFLXM and AAFLXM are binary files containing the angular forward and adjoint fluxes respectively at each fine-mesh boundary. SNCONS is a binary file containing the directional weights and cosines.

Table 1. Gamma 21 multigroup structure in MeV group boundaries.

Group	E(Top)	E(Low)	E(Mid-Point)
1	14.0	12.0	13.0
2	12.0	10.0	11.0
3	10.0	8.0	9.00
4	8.0	7.5	7.75
5	7.5	7.0	7.25
6	7.0	6.5	6.75
7	6.5	6.0	6.25
8	6.0	5.5	5.75
9	5.5	5.0	5.25
10	5.0	4.5	4.75
11	4.5	4.0	4.25
12	4.0	3.5	3.75
13	3.5	3.0	3.25
14	3.0	2.5	2.75
15	2.5	2.0	2.25
16	2.0	1.5	1.75
17	1.5	1.0	1.25
18	1.0	0.4	0.7
19	0.4	0.2	0.3
20	0.2	0.1	0.15
21	0.1	0.01	0.055

The S_n approximation to the multigroup contributon flux equation for group g is written as

$$C_g(r) = \int_{\hat{\Omega}} \left(\int_{\Delta E_g} \psi\left(r, E, \hat{\Omega}\right) dE \right) \psi^*(r, E_g, \hat{\Omega}) d\hat{\Omega} = \sum_{n=1}^{N} \omega_n \psi_{ng}(r)\, \psi_{-ng}{}^*(r) \tag{13}$$

where N is the total number of angular directions and ω_n is the direction weight for direction n. It should be noted that in equation (13) the adjoint flux must be taken in the opposite direction to the directions of forward flux. This is what $-n$ subscript stands for. It is not negative but signifies the opposite direction to n. Hence a discrete spatial representation of the contributon flux using 2D Cartesian geometry is written as

$$C_{i,j,g} = \sum_{n=1}^{N} \omega_n \psi_{i,j,n,g} \psi^*_{i,j,-n,g} \quad . \tag{14}$$

The definition of the contributon current in multigroup 2D Cartesian geometry is

$$D_{x,i,j}^{g} = \sum_{n=1}^{N} \omega_n \mu_n \psi_{i,j,g,n} \psi_{i,j,g,-n}^{*} \qquad D_{y,i,j}^{g} = \sum_{n=1}^{N} \omega_n \eta_n \psi_{i,j,g,n} \psi_{i,j,g,-n}^{*} \tag{15}$$

where n is the discrete direction index for forward flux, $-n$ direction opposite to direction n, i, j represent the index of the ij mesh point, N is the total number of discrete directions and g is the energy group number. The multigroup contributon flux and current are calculated at each mesh point.

In order to calculate the adjoint flux one needs to know the detector's response. The dose absorbed in the detector was chosen as a response. Therefore group dependent flux-to-dose conversion factors will play the role of the adjoint source. These factors are presented in Table 2 and are based on the relations found in reference 5.

Table 2. Flux-to-Dose conversion factors.

Group	Flux-to-Dose conversion factors (mrem/hr)/(n/cm^2-s)
1	1.118e-02
2	9.660e-03
3	8.189e-03
4	7.282e-03
5	6.957e-03
6	6.595e-03
7	6.195e-03
8	5.828e-03
9	5.458e-03
10	5.081e-03
11	4.698e-03
12	4.304e-03
13	3.895e-03
14	3.469e-03
15	3.010e-03
16	2.514e-03
17	1.955e-03
18	1.218e-03
19	5.606e-04
20	2.743e-04
21	1.367e-04

IV. Dipole Sample Problem

A simple, but illustrative, sample problem was used to verify the codes and demonstrate the basic concepts of the contributon theory. This problem represents a single source-detector symmetrically placed in a water plane. [6] The material densities are given in Table 3. The geometry of this problem is presented in Fig. 2. It contains a region 50 x 70 cm^2 filled with water. The region consists of 3500 fine meshes 50 x 70. The forward source is located at mesh points (21,24), (22,24), (21,25), and (22,25) and contains a 21 group photon source.

The detector located at mesh points (49,24), (50,24), (49,25), and (50,25) registers the dose rate. The dose rate in the detector is calculated by multiplying the total flux at the detector's location by the flux-to-dose conversion factor for each energy group.

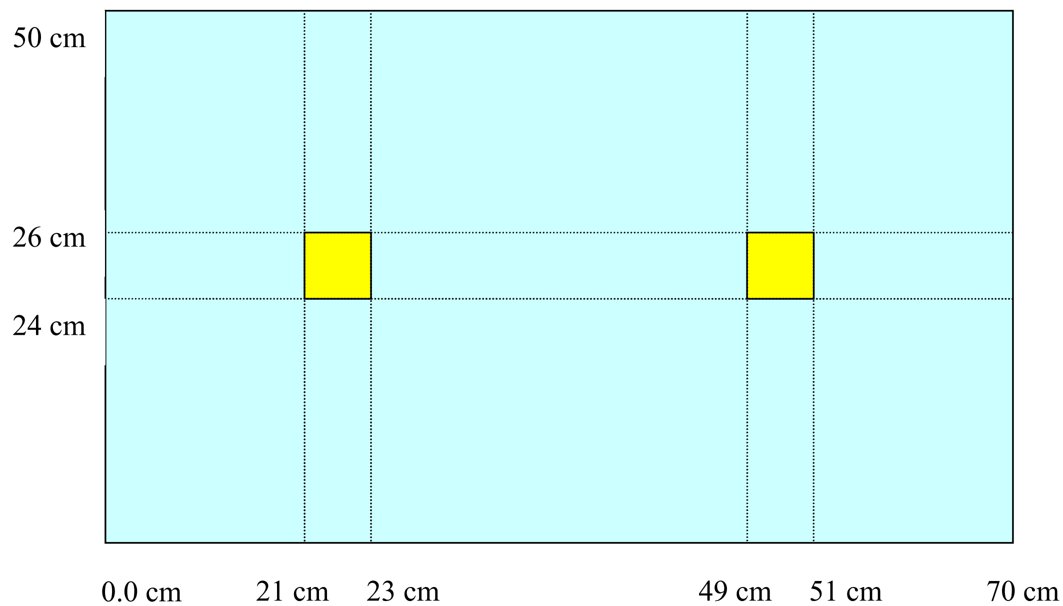

Figure 2. Sample dipole problem geometry.

Table 3. Material densities (atoms/b-cm) for the sample dipole problem.

Material	H_2O
O16	3.346E-2
H	6.691E-2

V. Preliminary Results

Several contributon theory calculations were performed for two cases based on the simple dipole problem from above. In the first case a simple dipole containing forward and adjoint sources are placed symmetrically in a region filled with water. The second case is the same as the base dipole problem except that it contains a shield region between the forward and adjoint sources. These are the same cases as found in reference [6].

The auxiliary post-processing codes CTBFLUX and CTBCURRENT were used to reconstruct the fluxes from the DANTSYS output files and they calculate the contributon flux and current, respectively. This data was then analyzed in MATLAB to help visualize the distribution of contributons across the area of the sample problem.

V.1 Case 1

Figure 3 represents the contributon flux with the forward source emitting photons only in group 21 (0.01-0.1 MeV). The detector registers the dose rate. As expected the figure is symmetric since the number of contributons that are emitted at the source location must reach the detector and be absorbed by it.

Figure 4 represents the contributon current for the source emitting photons in the 21st energy group. The plots of contributon current and contributon flux show that the response spreads out in the region between the forward and adjoint source points, but preferably flows along the straight path between the source and the detector.

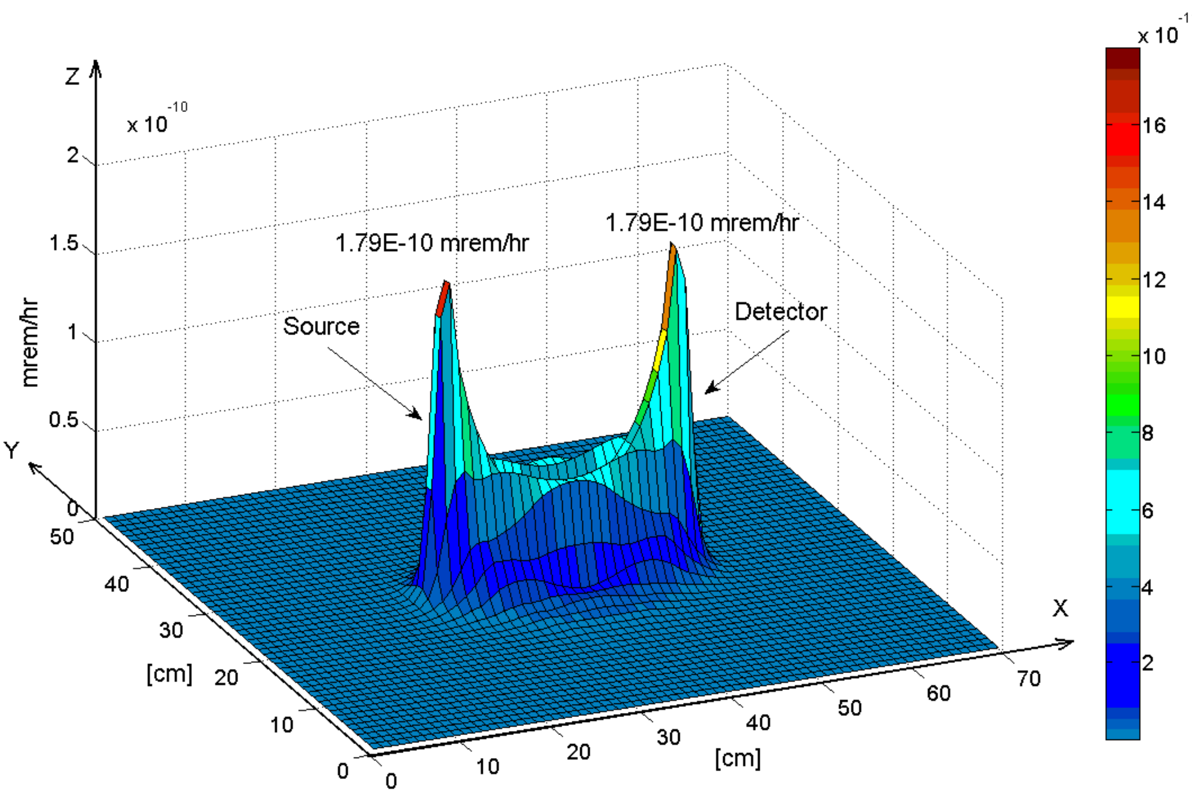

Figure 3. Group 21 contributon flux.

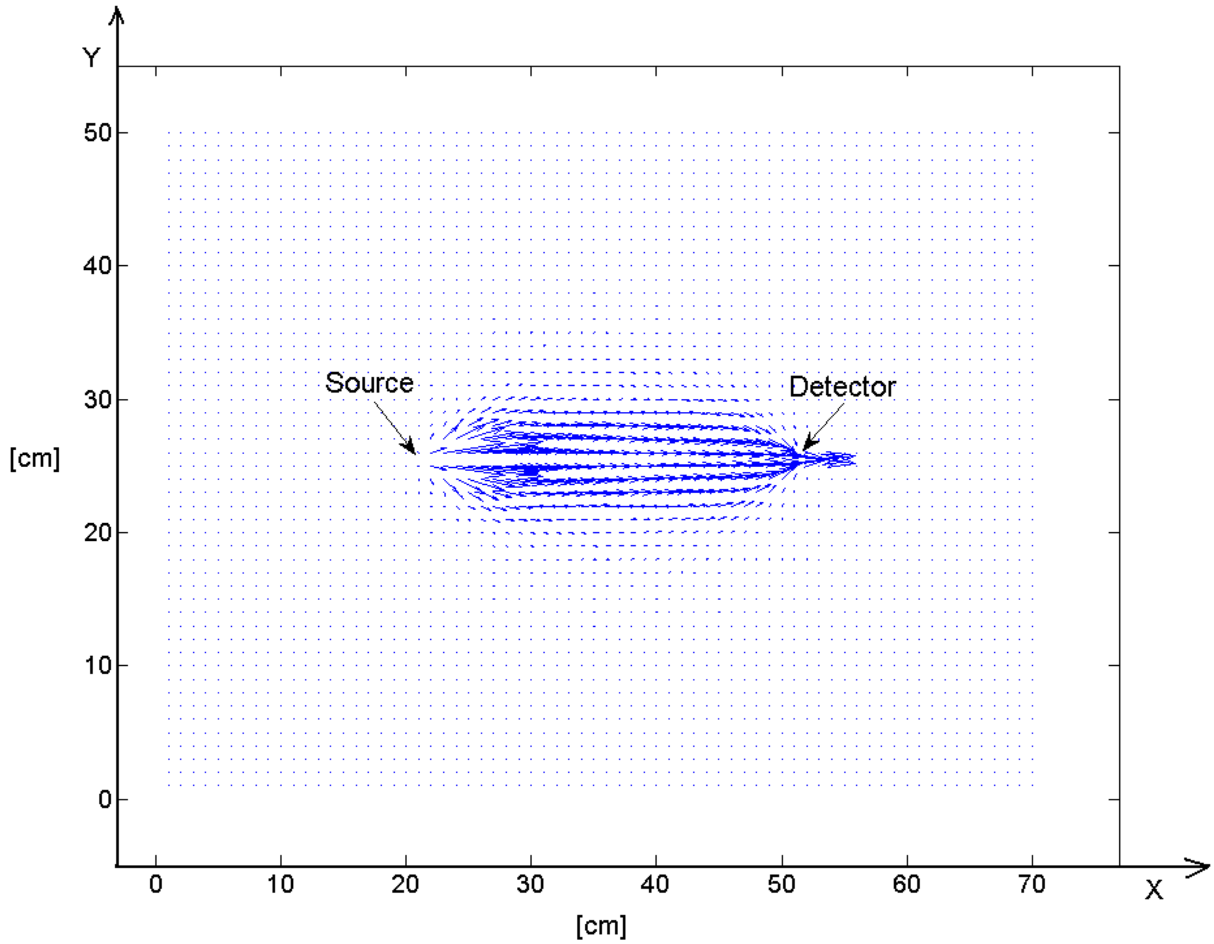

Figure 4. Group 21 contributon current.

The following figures Fig. 5 and Fig. 6 represent the contributon flux and contributon current for the source emitting the photons only in group number 10 (4.5-5 MeV). As the energy increases we start to observe unphysical oscillations in the contributon flux and current distribution. Such nonphysical behavior is referred to as the "ray effect". This effect happens because of the small ratio of scattering to total cross section and small dimensions of the model problem. Most of the photons are uncollided and the quadrature formula is unable to approximate the flux from the angular flux even though the angular flux may be exact at a fixed number of ordinates. This issue will be discussed later.

Figures 7 and 8 show the contributon flux and contributon current for the source emitting the photons with the highest energy – 1 group (12-14 MeV). As one can see the ray effect becomes even more pronounced for the source in the highest energy.

As a remedy for the "ray effect" the DANTSYS code has a so-called First Collision Source option. Using this option for the source emitting photons in the 1st group we get the contributon flux distribution presented in Fig. 9. The flow of contributon current is presented in Fig. 10. As one can see the distribution in this case loses its symmetry. The reason of this asymmetry is, probably,

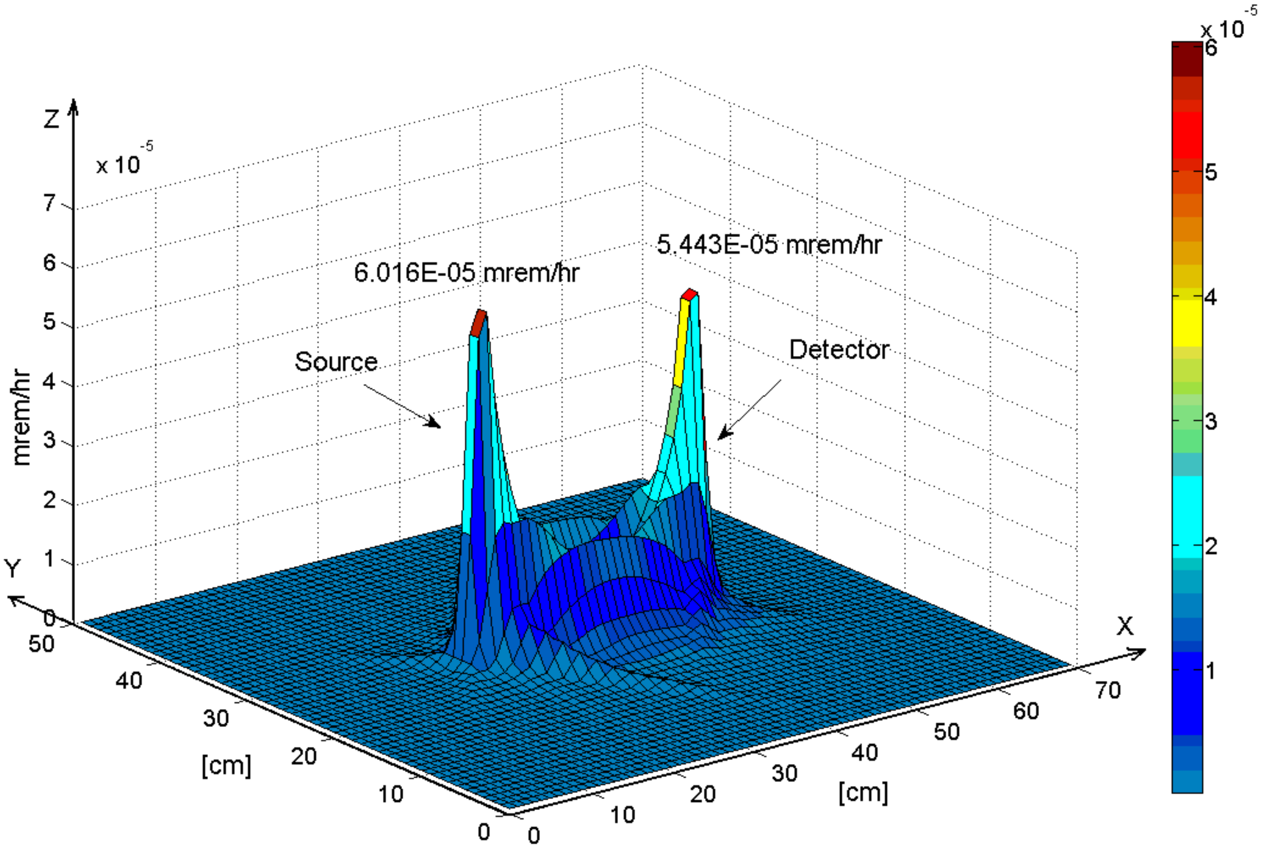

Figure 5. Group 10 contributon flux.

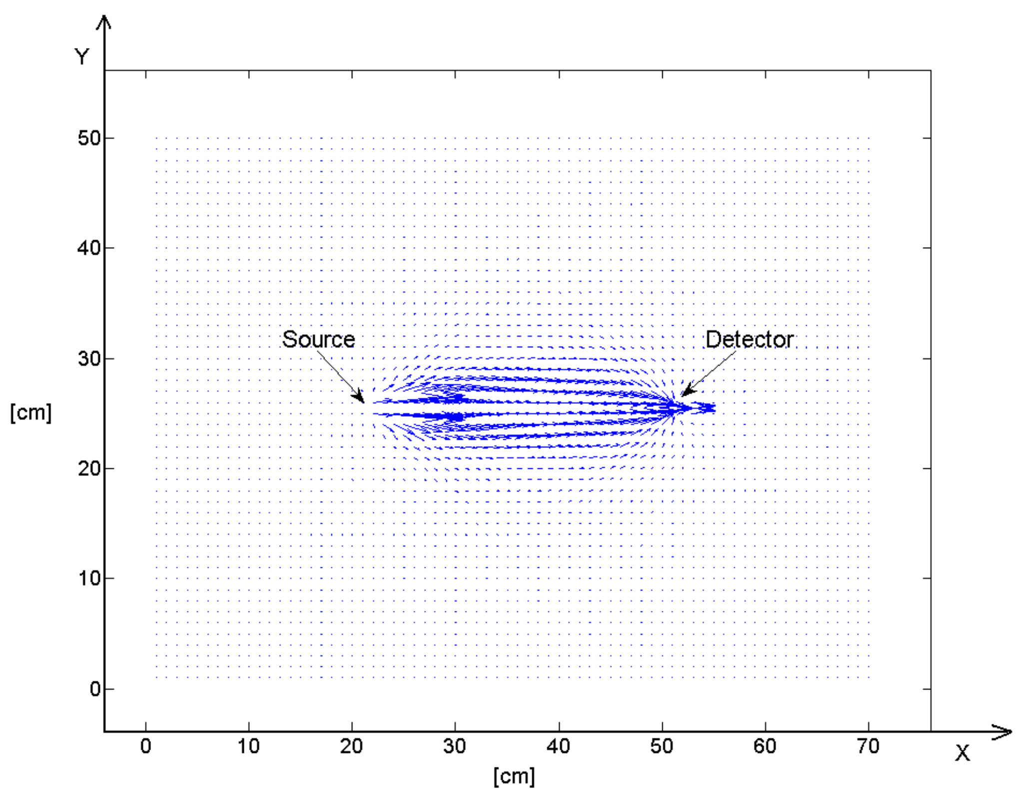

Figure 6. Group 10 contributon current.

because of the following: In contributon theory the value $\psi^*(r,E,\Omega)\,Q(r,E,\Omega)$ is called the contributon response source, where $Q(r,E,\Omega)$ is the forward source. The value $\psi(r,E,\Omega)\,Q^*(r,E,\Omega)$ is called the contributon response sink. The contributons originate at the response source and they flow out at the response sink. Now for the First Collision Source option the forward source is located not only in the source location itself but also at the photon's first collision sites all across the area of the dipole problem. But the response sink is still in the area of the detector. Therefore contributons originating from the source plus at the other places of the region must flow out the response sink, which is the detector itself. Therefore the value of the peak on the detector side is higher than the peak on the source side.

The dose rate distribution inside the detector has been calculated. The detector consists of four cells. The schematic of the detector and the coordinates of each detector's cell are presented in Fig. 11.

The dose rates in each cell of the detector for energy groups 1, 10, 21 and group 1 with the First Collision Source option are presented in Table 4. Since photons are entering the detector from the side of cells 1 and 3 along the direction X it is expected that cells 1 and 3 have equal dose rates and cells 2 and 4 have equal does rates. This can be seen from Table 4 with slight deviation from this rule for First Collision Source option.

The other way to eliminate the "ray effect" is to use a Monte Carlo based transport code. This option currently is work in progress.

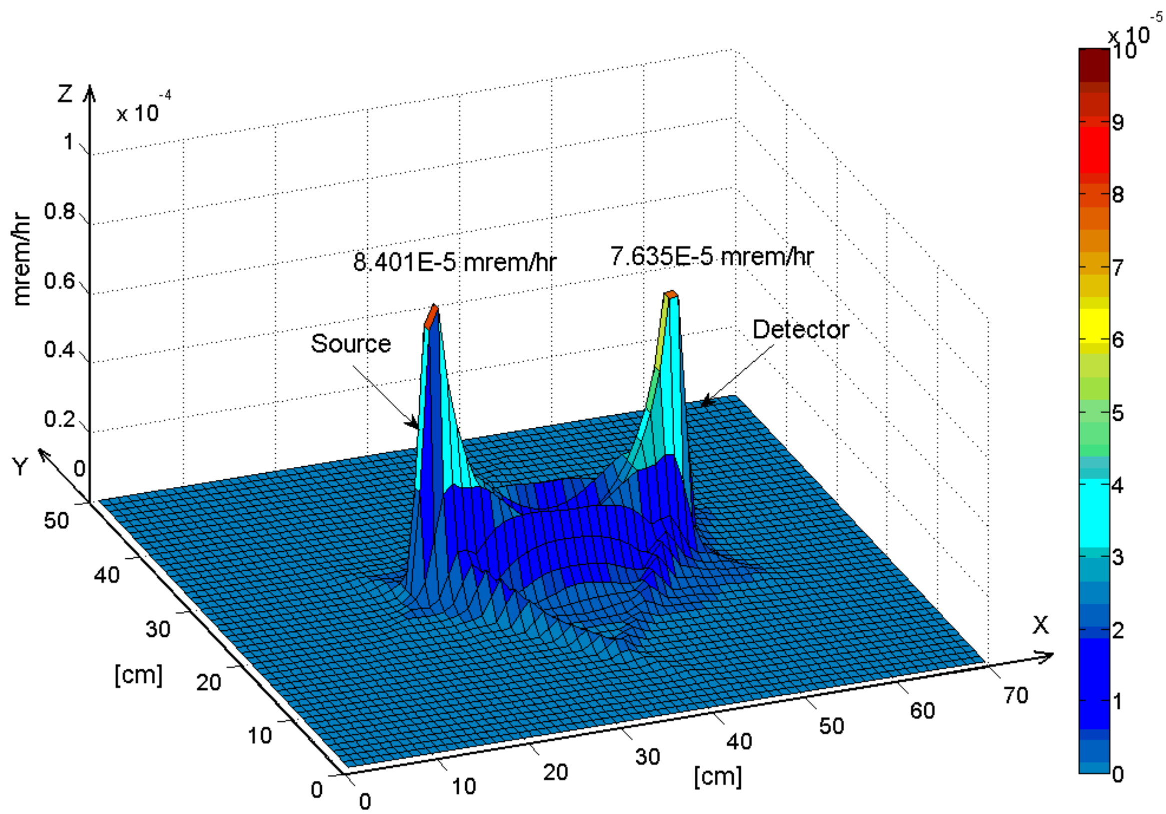

Figure 7. Group 1 contributon flux.

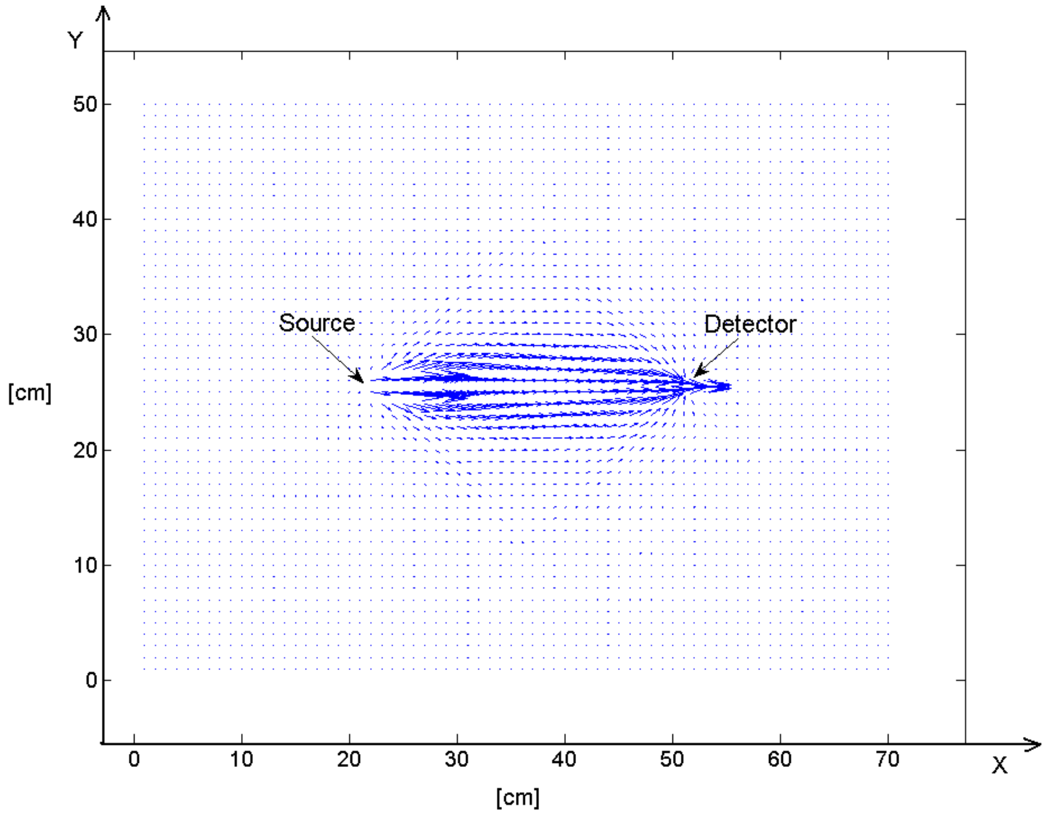

Figure 8. Group 1 contributon current.

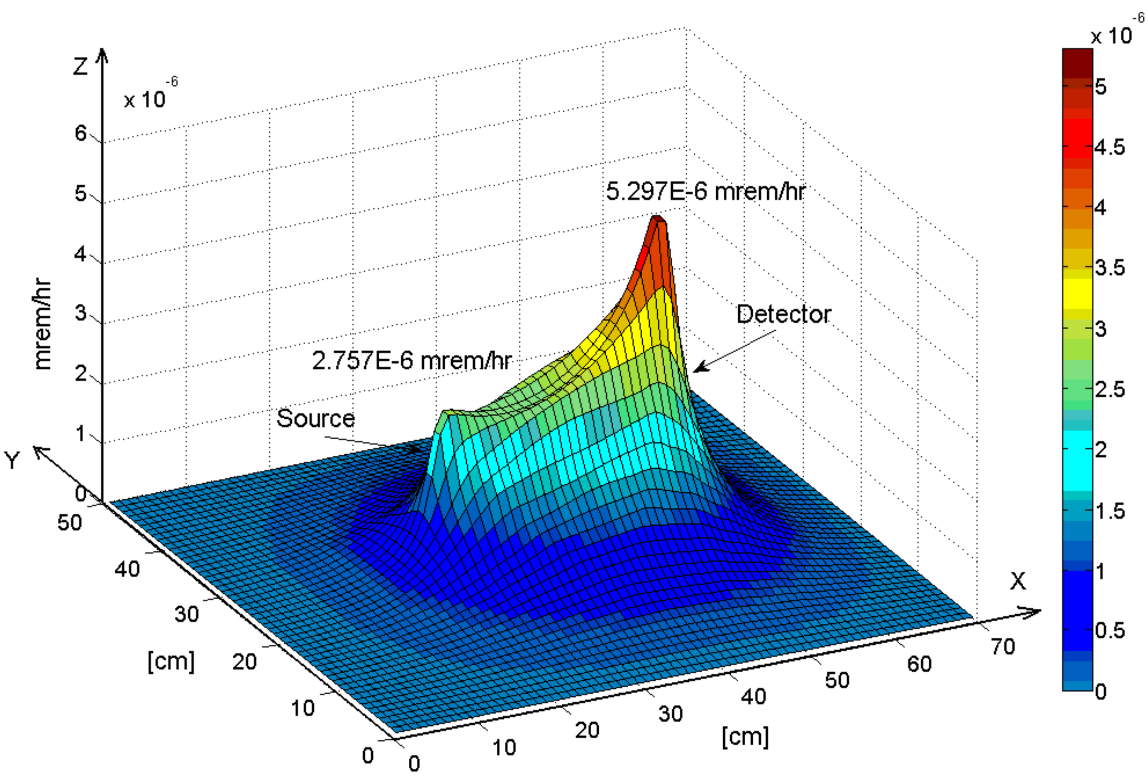

Figure 9. Group 1 contributon flux with First Collision Source option.

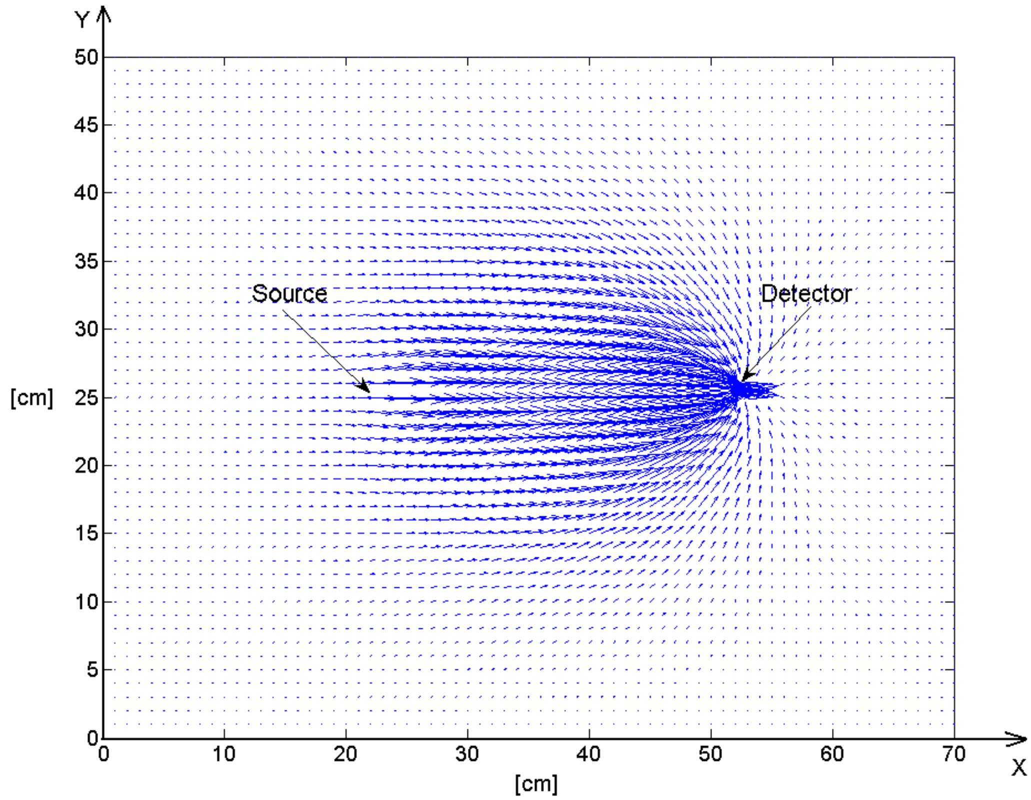

Figure 10. Group 1 contributon current with First Collision Source option.

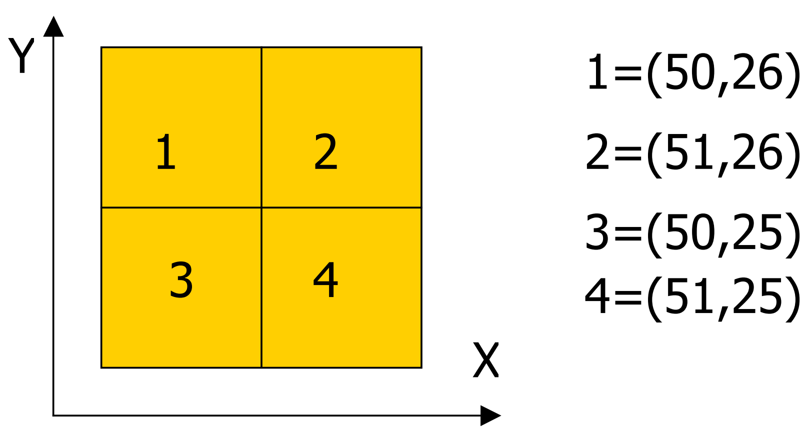

Figure 11. Detector

Table 4. Dose rate distribution in the detector.

Group\Cell	1	2	3	4
1	3.93E-05	3.72E-05	3.93E-05	3.72E-05
10	2.94E-05	2.79E-05	2.94E-05	2.79E-05
21	1.19E-10	7.82E-11	1.19E-05	7.82E-11
1 with FCSRC option	1.89E-04	1.77E-04	1.87E-04	1.79E-04

In order to verify the conservation of the contributons the response flows across the surfaces 1 and 2 as shown in Fig. 12 were calculated and compared to the integral response of the detector. The results are presented in Table 5. It shows that the difference between fluxes across the surfaces 1, 2 and detector's response is less than 2% for 1st and 10th energy groups. For the 21st energy group the difference increases up to 5%. This is probably because the multiplication of the forward and adjoint fluxes increases the computational error compared to the error in the forward or adjoint fluxes alone. The difference in the case with the First Collision Source option is quite large – more than 40 times. This means that there is a problem with the rtflux binary file for the first collided source method. Not all the flux data is stored within it. Obtaining the results for the first collided source method will need to be resolved differently.

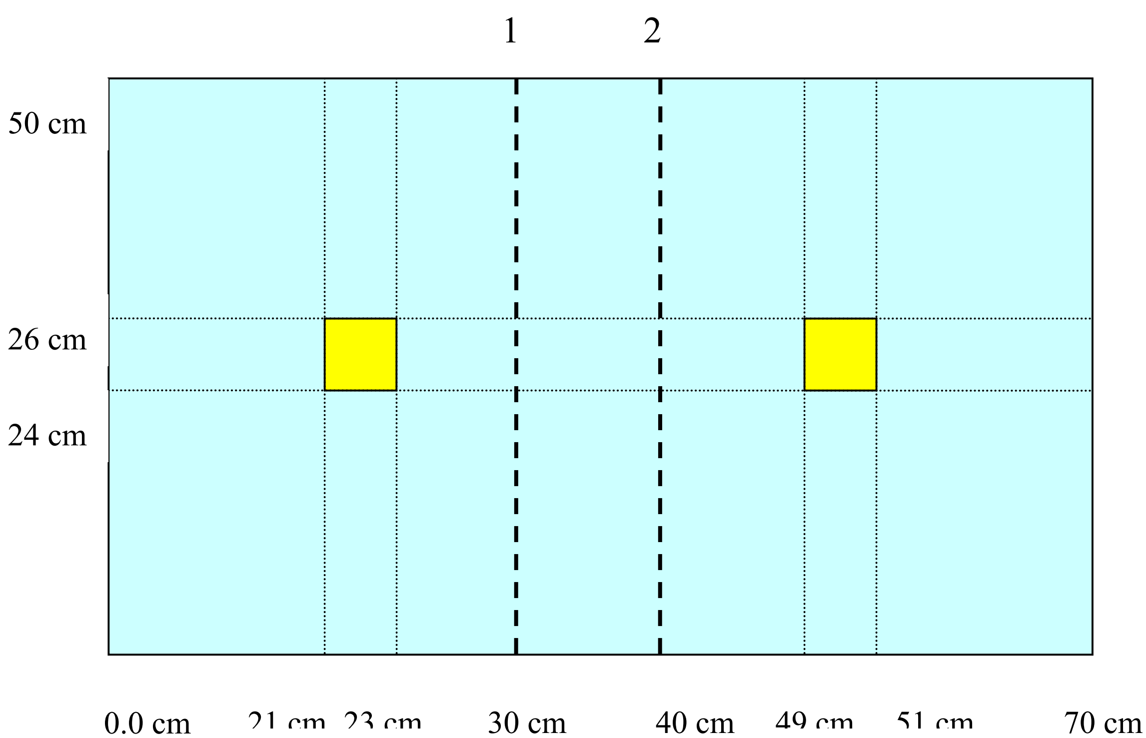

Figure 12. Dipole problem with test surfaces 1 and 2.

Table 5. Response flow calculations in comparison with the detector response.

Energy group	Response flow across the surface 1 (mrem/hr)	Response flow across the surface 2 (mrem/hr)	Integral detector response (mrem/hr)
1	1.50E-04	1.49E-04	1.53E-04
10	1.14E-04	1.13E-04	1.15E-04
21	4.16E-10	4.15E-10	3.94E-10
1st group with First Collision Source option	1.76E-05	2.88E-05	7.36E-04

V.2. Case 2

For the second test case the lead shield has been introduced between the forward and adjoint sources as shown in Fig. 13

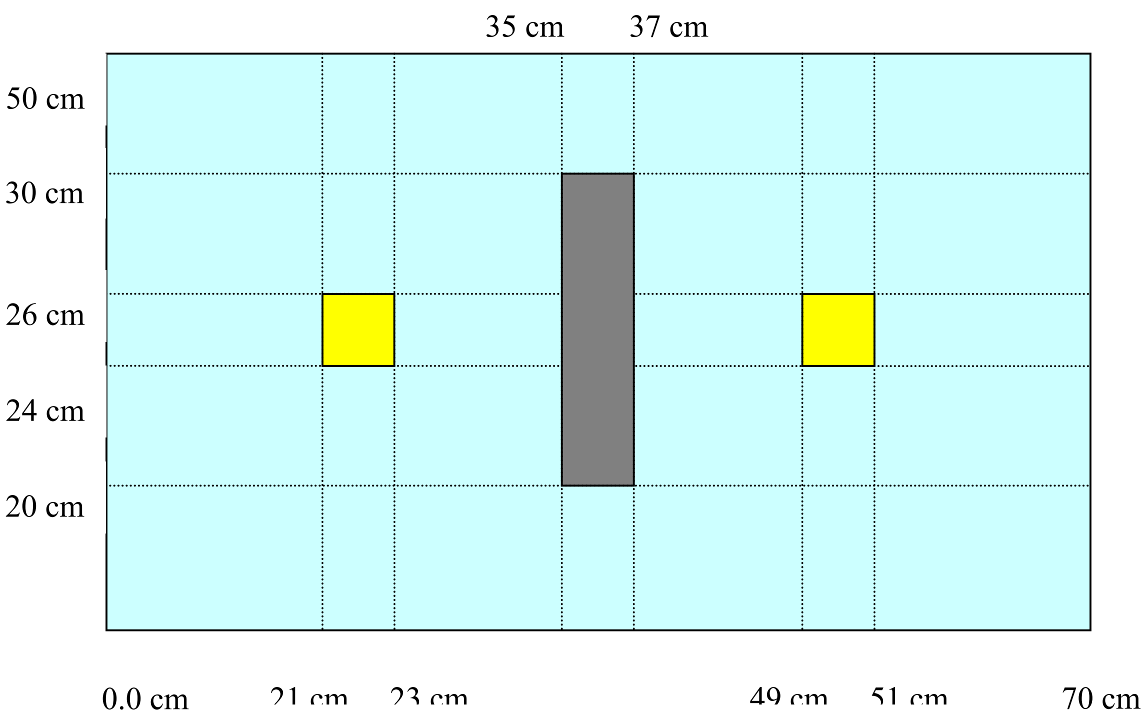

Figure 13. Sample dipole problem with the shield.

All the steps that have been performed for the simple dipole problem are repeated for the problem with the shield. The following figures present the contributon flux and current for the source emitting the photons of the last energy group.

A comparison of Fig. 14 and Fig. 15 with Fig. 3 and Fig. 4 shows that the flow of contributons decreases across the lead shield and increases around the shield. Fig. 14 and Fig. 15 describe how the contributons are flowing around the shield. The follow paths are clearly seen on the current plot.

The next figures are for the higher energy groups. Figures 16 and 17 represent the contributon flux and current respectively for the 10th energy group. Figures 18 and 19 show the contributon flux

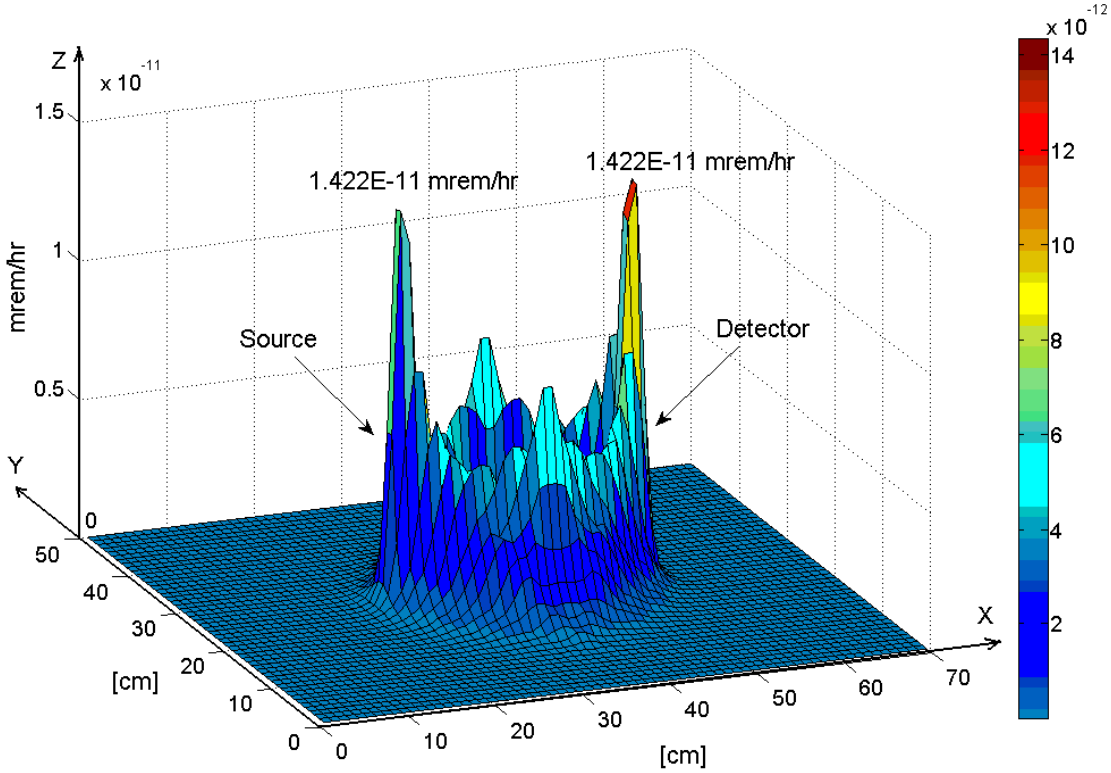

Figure 14. Group 21 contributon flux.

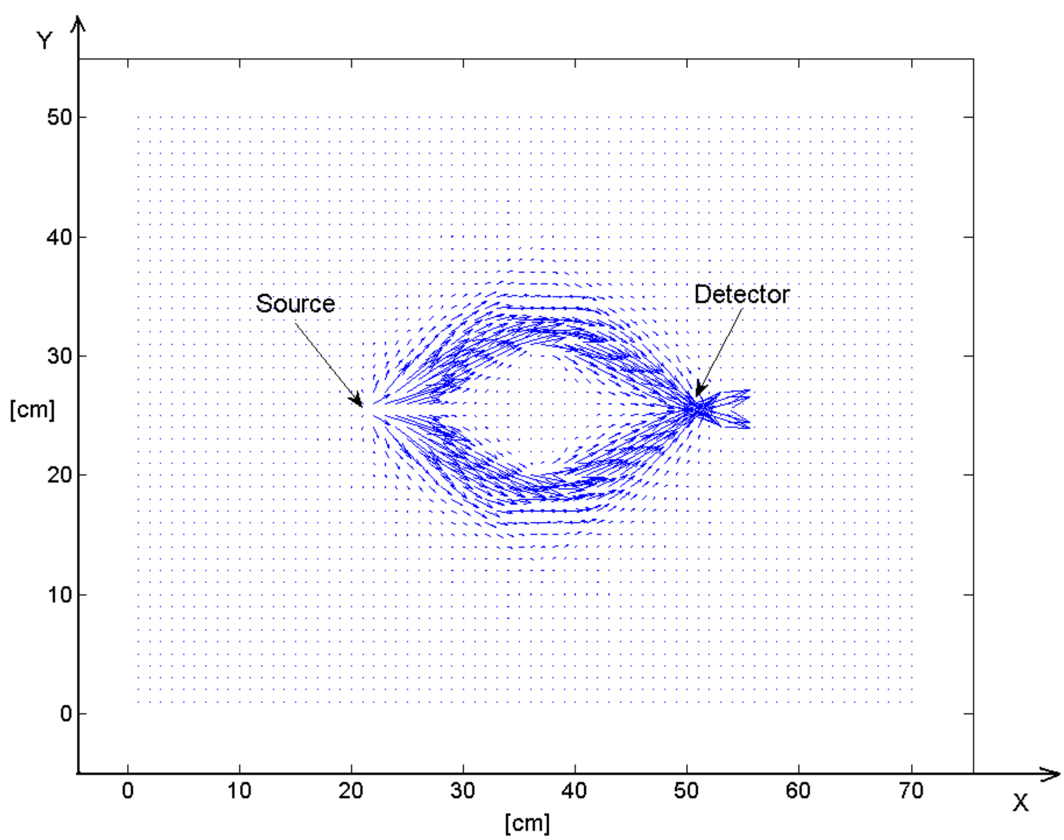

Figure 15. Group 21 contributon current.

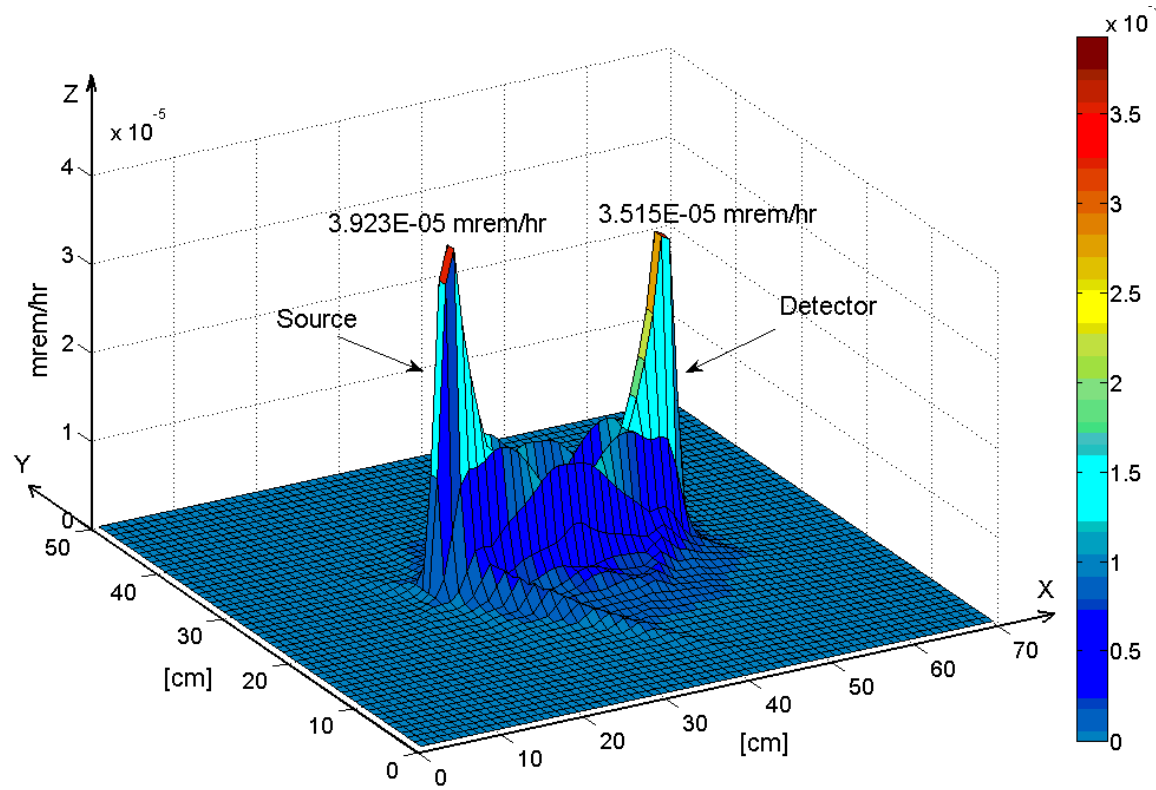

Figure 16. Group 10 contributon flux.

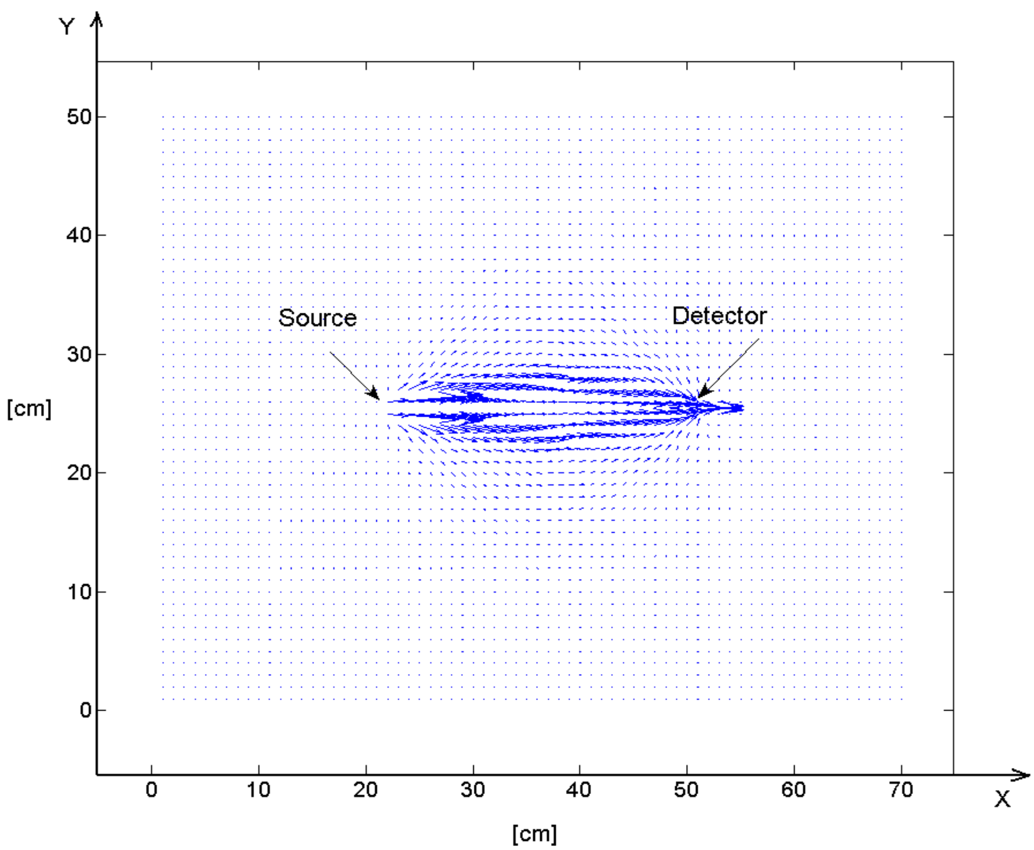

Figure 17. Group 10 contributon current.

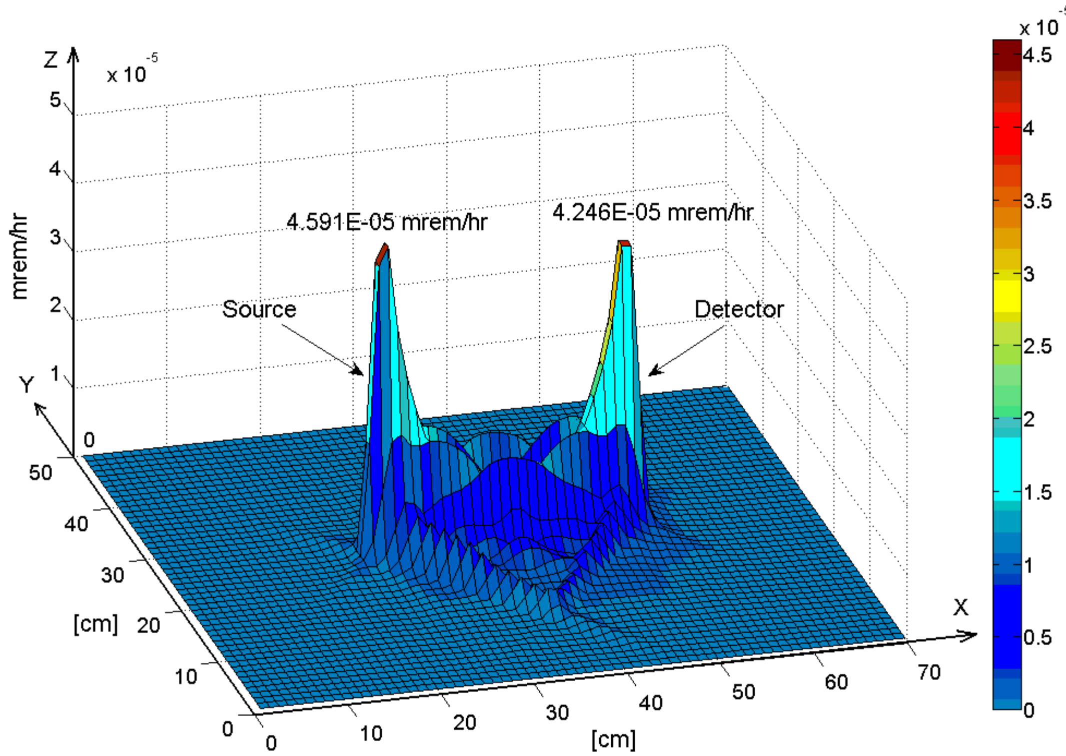

Figure 18. First Group contributon flux.

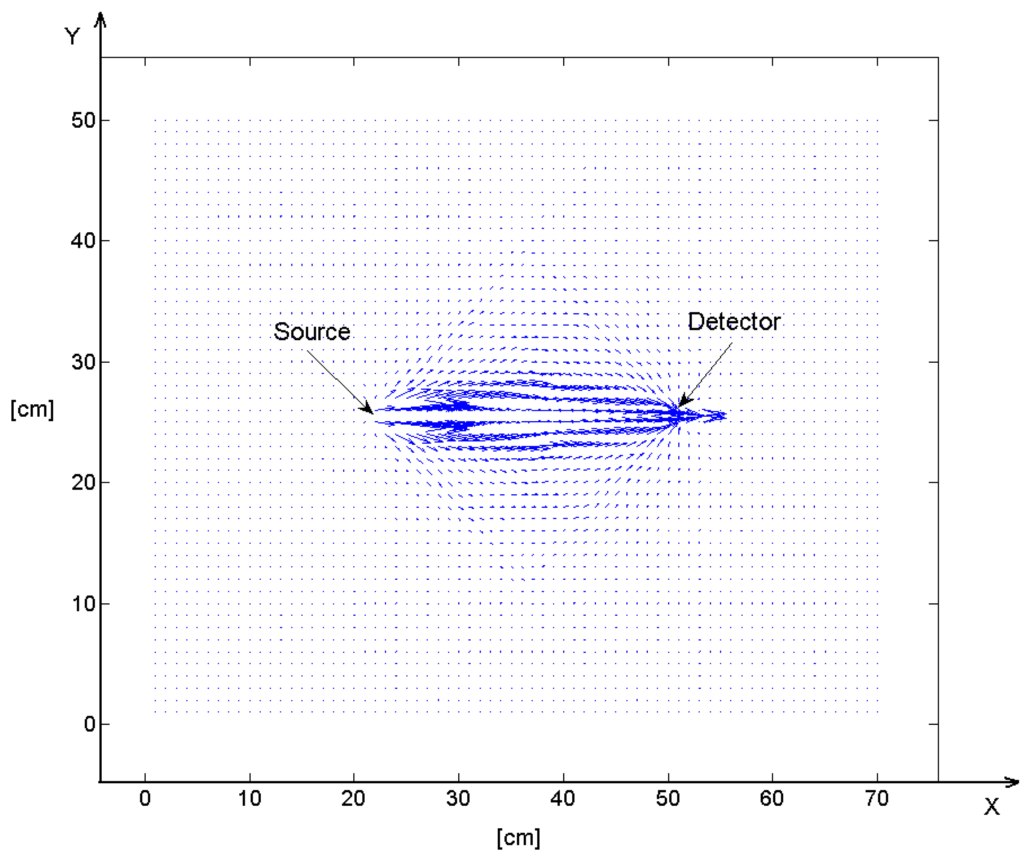

Figure 19. First Group contributon current.

and current respectively for the first energy group. As these figures show the higher the energy of the photons the more they penetrate the shield. The flow lines become straighter in comparison with the flow lines for the last energy group.

The same type of dose calculation as in case 1 has been done for the case with the shield. The total contributon flow through the surfaces at x=30 cm and x=40 cm is calculated and compared with the integral detector's response. The results are presented in Table 6. Similarly to the results of Table 5, the contributon flow through the surfaces is close to the total dose in the detector except for the case of using First Collision Source option for the first group.

Table 6. Response flow calculations in comparison with the detector response.

Energy group	Response flow across the surface 1 (mrem/hr)	Response flow across the surface 2 (mrem/hr)	Integral detector response (mrem/hr)
1	8.58E-05	8.63E-05	8.86E-05
10	7.57E-05	7.54E-05	7.70E-05
21	3.88E-11	3.93E-11	3.60E-11
1st group with First Collision Source option	1.3E-05	1.98E-05	2.19E-04

VI. Sample Problem with a Duct

Another sample problem was used to verify the codes and demonstrate the basic concepts of the contributon theory. A similar but three-dimensional case is found in reference [7]. The problem represents a 50 x 50 cm^2 concrete shield slab containing a three-legged duct filled with air. The material densities are given in Table 7. The duct has a width of 10 cm with its entrance centered at the front face. The geometry of this problem is presented in Fig. 20. The region consists of 2500 fine meshes, the forward source is 2×2 cm^2 and located at mesh points (1,15), (1,16), (2,15), and (2,16) and contains a 21 group photon source. The detector is 2×2 cm^2 and located at mesh points (49,35), (49,36), (50,35), (50,36). The dose rate in the detector is calculated by multiplying the total flux at the detector's location by the flux-to-dose conversion factor given in Table 2 for each energy group.

Table 7. Material densities for the sample duct problem.

Material	Density
Concrete	[atoms/b-cm]
O	4.3E-2
H	1.04E-2
C	6.459E-3
Si	7.8E-3
K	2.68E-4
Ca	8E-3
Fe	2.05E-4
Na	2.55E-4
Mg	8.51E-4
Al	1.067E-3
N	1.0E-5
S	7.4E-5
Ti	1.5E-5
Steel	
C	7.96E-4
Si	4.25E-4
Mn	3.91E-4
Fe	8.47E-2
Water	
H^1	6.6856E-2
H^2	1.0030E-5
O	3.3433E-2

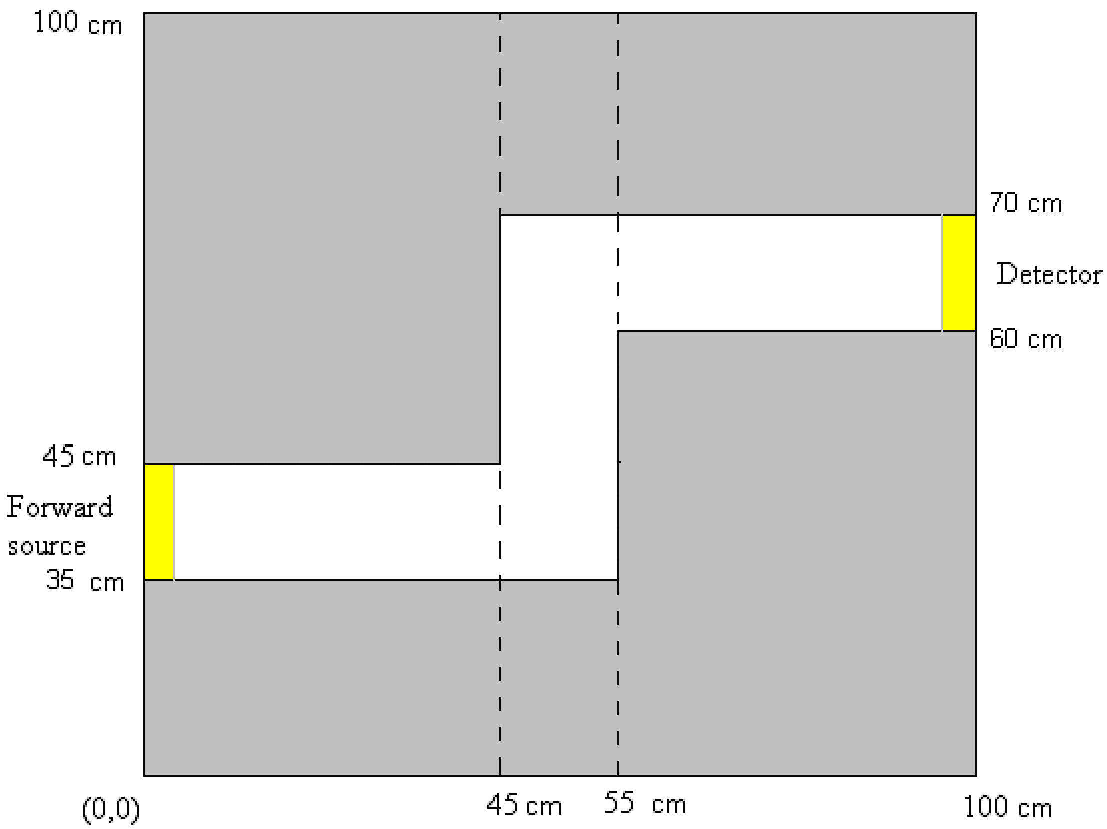

Figure 20. Sample duct problem with geometry.

VII. Preliminary Results

Several contributon theory calculations were performed for the duct case. The auxiliary post-processing codes were used to reconstruct the fluxes from the DANTSYS output files and calculate the contributon flux and current. This data was then analyzed in MATLAB to help visualize the distribution of contributons across the area of the sample problem. Figure 21 represents the contributon flux with the forward source emitting photons only in group 1 (12-14 MeV). Figure 22 represents contributon current for the same energy group. As one can see, photons travel almost in a straight line with slight scattering from the boundaries of the duct.

The next two figures (Fig. 23 and Fig. 24) represent contributon flux and current for photons emitted in energy group 16 (1.5-2 MeV). As the energy of the photons becomes lower, scattering plays a more significant role. The flow path depicted in Figure 24 is wider than in Figure 21 due to an increase in scattering of photons before they reach the detector.

The final two figures (Fig. 25 and Fig. 26) show contributon flux and current of photons in the lowest group 21. As it is expected the low energy photons that contribute to the detector's response go exactly along the duct. This is because the mean free path of these photons in concrete is considerably shorter than the distance from source to detector and much shorter than the mean free path in air. Therefore low energy photons reach the detector by scattering from the concrete wall back into the duct filled with air.

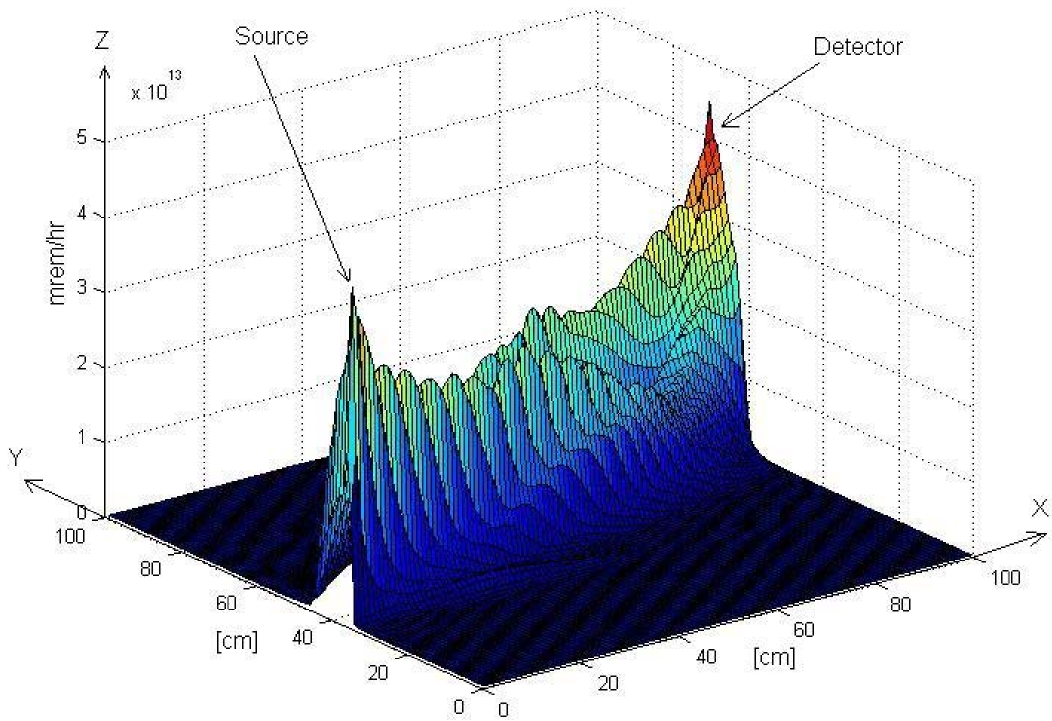

Figure 21. First Group contributon flux.

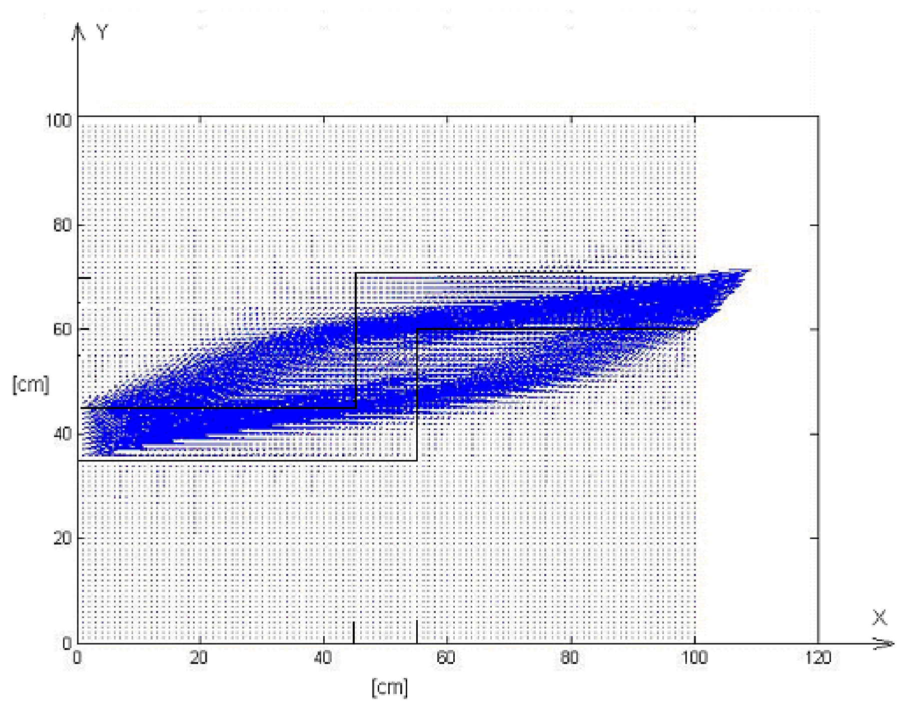

Figure 22. First group contributon current.

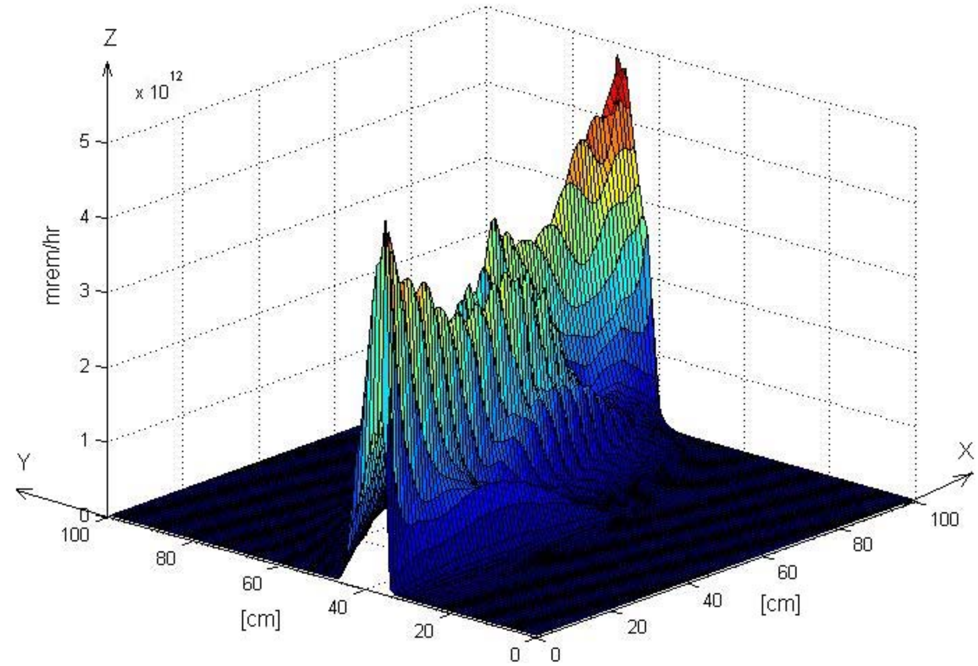

Figure 23. Group 16 contributon flux.

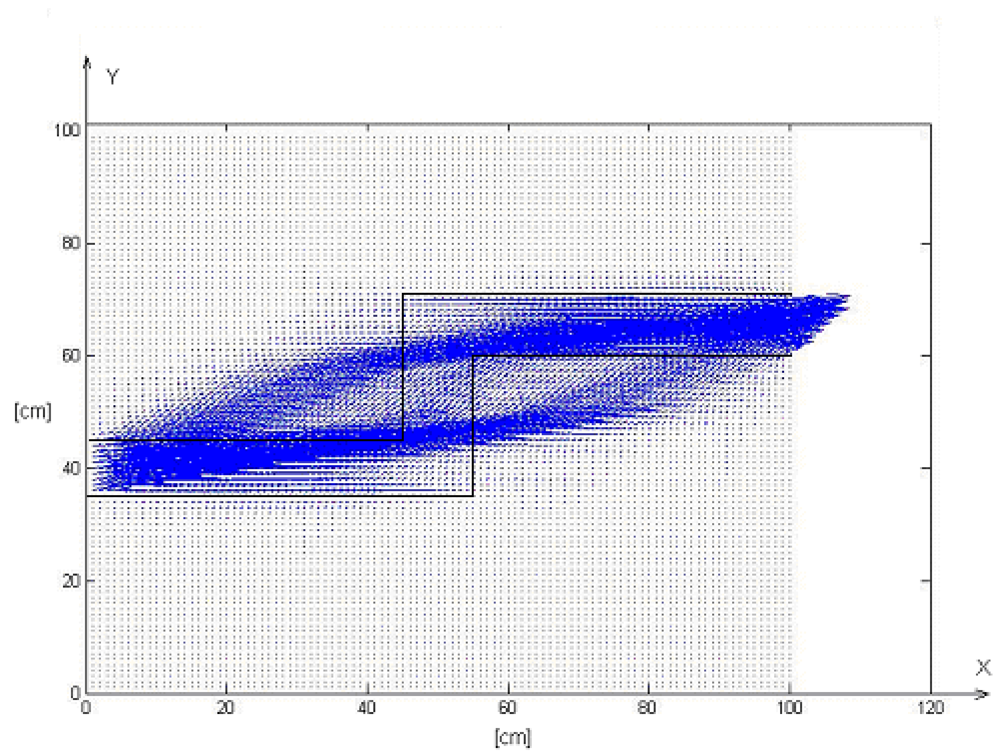

Figure 24. Group 16 contributon current.

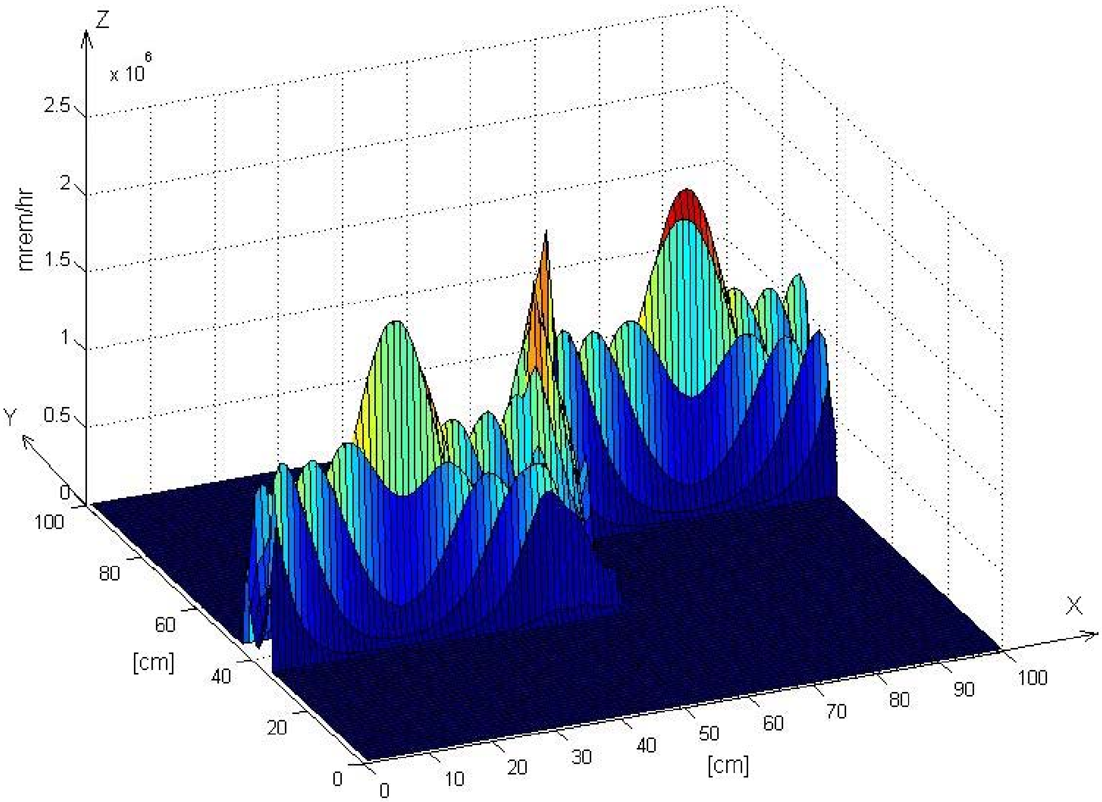

Figure 25. Group 21 contributon flux.

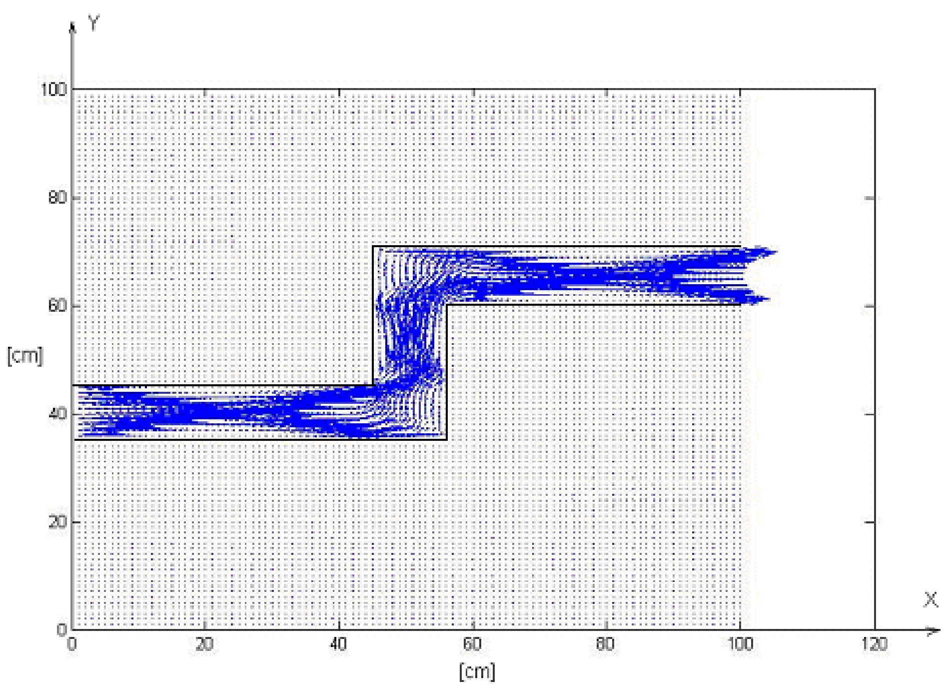

Figure 26. Group 21 contributon current.

In order to find out what the contribution from each energy group is to the detector, a computation of the same problem was performed with the following parameters:

1) Forward source was emitting photons only in Group 16 (1.5-2 MeV)
2) Computation of adjoint problem was performed 6 times with the sensitivity of the detector only for one energy group, or in other words each adjoint problem had an adjoint source only in one group, from group 16 (1.5-2 MeV) to group 21 (0.1-0.01 MeV).

The histogram in Figure 27 represents the contribution of each photon energy group to the total dose rate.

It is interesting to note that the highest fraction of the dose rate registered by the detector comes from photons downscattered into group 19 (0.4-0.2 MeV).

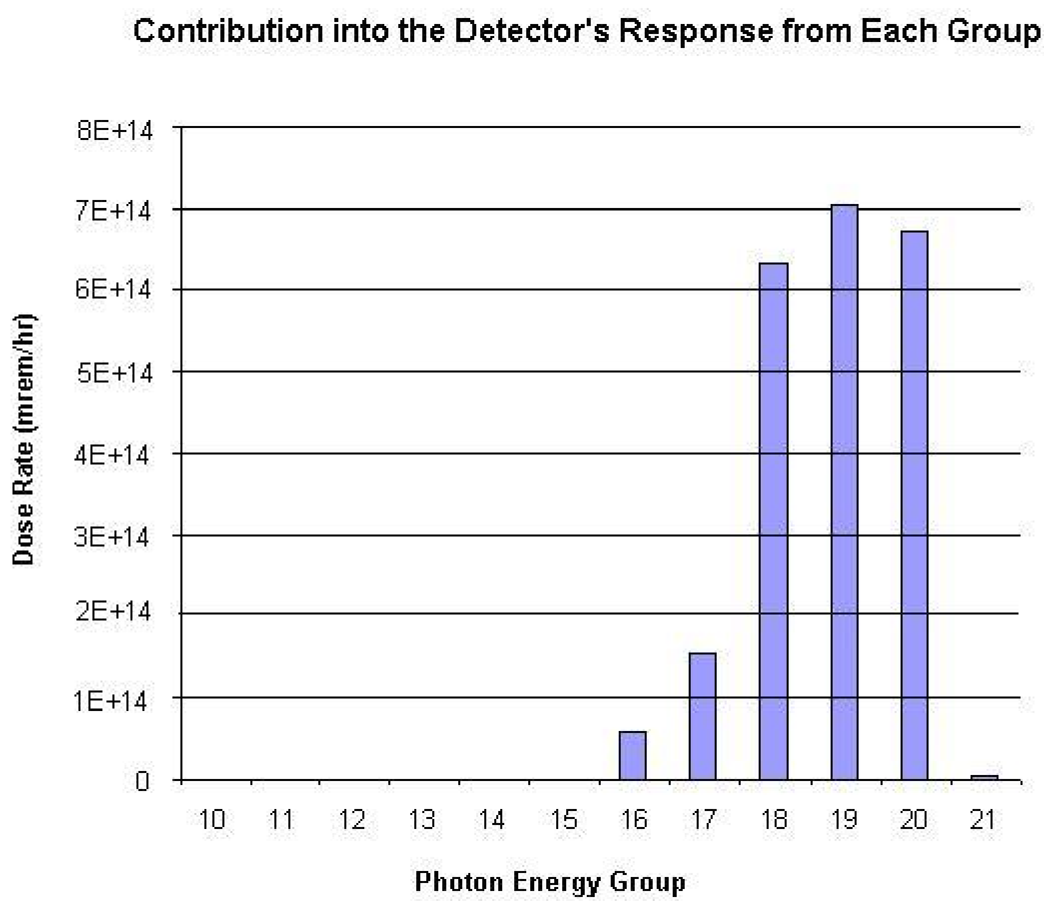

Figure 27. Contribution of each energy group to the detector from the photon with initial energy in group 16 (1.5-2 MeV).

VIII. Conclusion

The neutron/photon transport code DANTSYS has been used to calculate the forward and adjoint photon fluxes. A contributon code has been developed. The code uses the angular forward and adjoint fluxes from the DANTSYS output files to calculate the contributon theory parameters, which are contributon flux and contributon current. The demonstration and verification was done with two problems: (1) a dipole problem and (2) a duct problem using a 21 group photon cross section library, flux-to-dose conversion factors and source. The auxiliary post-processing contributon codes have been applied to two cases of a dipole problem: first is a simple dipole problem and second is a dipole problem with a shield between source and detector. Also it was applied to a three-legged duct problem. The data was processed in MATLAB for visualization. The results show the conservation of the contributon in the system. The contributon flow into the system is equal to the contributon drain out of the system. The other thing the results show is fluid like behavior of the contributons. This can especially be seen in the problem with the shield between the source and detector and in the three-legged duct problem.

For the higher energy photons the limitation of the S_n method called "ray effect" has been observed. This effect arises in problems that have very little scattering and localized source. Unfortunately, the built-in remedy for the ray effect using the First Collision Source option does not give satisfactory results. To avoid this problem the use of code based on Monte Carlo transport is considered for future work.

References

1. M.L. Williams "Generalized Contributon Response Theory", Nuclear Science and Engineering. 108, 355-383 (1991)

2. M.L. Williams, H. Manohara, "Contributon Slowing Down Theory", Nuclear Science and Engineering, 111, 345-367 (1992)

3. E.E. Lewis and W. F. Miller, "Computational Methods of Neutron Transport", American Nuclear Society, Inc., La Grange Park, Illinois (1993)

4. R.E. Alcouffe, R.S. Baker, F.W. Brinkley, D.R. Marr, R.D. O'Dell, and W. F. Walters, "DANTSYS: A Diffusion Accelerated Neutral Particle Transport Code System," Los Alamos National Laboratory report LA-12969-M (1995)

5. American National Standard Neutron and Gamma-Ray Flux-to-Dose-Rate Factors, ANS/ANS-6.1.1-1977 (N666)

6. E. Gungordu "Visualization of two dimensional particle transport calculations with the use of generalized contributon theory", Abstract of thesis submitted for the MS degree, University of Massachusetts Lowell, July (1997)

7. I.K. Abu-Shumays, M.A. Hunter, R.L. Martz, and J.M. Risner "Generalization of Spatial Channel Theory to Three-Dimensional x-y-z Transport Computation", Bettis Atomic Power Laboratory, March 12 (2002)